

Synthesis and Optical Properties of Ce-doped ZnO

YANG Jing-hai^{1,2,3*}, GAO Ming¹, ZHANG Yong-jun¹, YANG Li-li^{1,2}, LANG Ji-hui^{1,3},
WANG Dan-dan², WANG Ya-xin¹, LIU Hui-lian^{1,2}, FAN Hou-gang¹,
WEI Mao-bin¹ and LIU Fu-zhu¹

1. The Institute of Condensed State Physics, Jilin Normal University, Siping 136000, P. R. China;

*2. Key Laboratory of Excited State Processes, Changchun Institute of Optics, Fine Mechanics and Physics,
Chinese Academy of Sciences, Changchun 130033, P. R. China;*

3. School of Material Science and Engineering, Jiangsu University, Zhenjiang 210013, P. R. China

Abstract ZnO nanorods were synthesized using the sol-gel method, and the effects of annealing temperature and Ce doping on the morphologies and optical properties of ZnO nanostructures were investigated in detail. The XRD measurements showed that the as-synthesized ZnO nanostructures had a hexagonal wurtzite structure. SEM images showed that uniform nanorods formed at 900 °C. Photoluminescence measurements showed an ultraviolet emission peak and a relatively broad visible light emission peak for the samples sintered at different temperatures. The UV emission peak bathochromically shifted when the annealing temperature rose from 850 to 1000 °C. Ce doping decreased the synthesized temperature of the ZnO nanorods to 500 °C, and the UV peaks hypsochromically shifted.

Keywords Annealing temperature; Ce-doped ZnO; Optical property

1 Introduction

Since the report that ZnO UV excited the luminescence in 1996, and the article “Will UV Laser Beat the Blue?” was published in “Science”^[1], the ZnO UV luminescence has been a much sought after research area. ZnO is attracting much attention, in addition to GaN, as a promising candidate for optoelectric application because of its excellent chemical and thermal stability and its specific electrical and optoelectronic property. In recent times some scholars and scientists have primarily aimed at using ZnO for optoelectronic application in the blue and ultraviolet(UV) light, for example, light emitting diodes, laser diodes, and UV detectors^[2,3]. Besides the UV light-emitting properties, visible luminescence in a range of 400—700 nm for ZnO, was also studied widely because of the potential application in low-voltage field emissive display^[4]. ZnO doped with selective elements usually offers an effective method to adjust the electrical and optical properties to get high emission efficiency. Although numerous experiments were performed to study the

synthesis and optical properties of Rare-earth(RE)-doped ZnO films or powders, little study was done on the RE-doped ZnO nanorods.

To date, it is still limited to fabricating a system of Ce-doped ZnO nanostructure, although there have been reports about Ce-doped 1D ZnO nanostructures and Ce-doped ZnO films by spray pyrolysis^[5,6]. Therefore, the authors have chosen Ce as a dopant/activator, because of the similar facet space of ZnO and CeO. In this article undoped and Ce-doped ZnO nanostructures have been fabricated by the sol-gel method. The as-prepared samples have been annealed at different temperatures from 850 to 1000 °C in ambient air. The effects of annealing temperature and cerium doping on the morphology, structure, and photoluminescence of ZnO nanostructures have been investigated systematically.

2 Experimental

Zinc nitrate hexahydrate reacted with citric acid in an equimolar ratio of 0.01 mol/L. Doping was per-

*Corresponding author. E-mail: jhyang@jlnu.edu.cn

Received November 9, 2007; accepted January 15, 2008.

Supported by the National Natural Science Foundation of China(No.60778040), the Hi-tech Research and Development Program of China(No.2007AA032400448), the Science and Technology Bureau of Jilin Province(No.20060518), Gifted Youth Program of Jilin Province(No.20060123), the Science and Technology Office of Education of Jilin Province(No.2007162), and the Science and Technology Bureau of Key Program for Ministry of Education(No.207025).

formed by adding 0.04 mol/L ethylene glycol to produce ZnO nanostructures. For the production of pure ZnO nanostructures, all reagents were of analytical grade and no further purification was needed. The mixed solution was stirred for 2 h, and then kept in a drying cabinet for some hours to form a dry gel. The dried gel was kept in a box furnace at 400 °C, for 1 h, to get an amorphous precursor of Zn—C—O composite powder. Then this precursor was sintered under 900 °C for 13 h. Finally the white powders were obtained after cooling down to room temperature. For the production of Ce-doped ZnO nanorods, it was performed by adding cerium nitrate hexahydrate to the previously mentioned mixed solution and the same drying process was performed to get a dried gel. The molar ratio of Ce to Zn was 2%. The dried gel was sintered at 500 °C for 6 h to get Ce-doped ZnO nanorods. To characterize the ZnO nanostructure, the XRD pattern was measured on a D/max-RA XRD spectrometer with a Cu $K\alpha$ line of 0.15406 nm. The surface morphology was studied with a SEM(Hitachi, S-570). PL measurement was performed on an HR800 LabRam Infinity Spectrophotometer, excited by a continuous He-Cd laser at a wavelength of 325 nm and a power of 50 mW.

3 Results and Discussion

3.1 Crystal Structure and Surface Morphology

The XRD patterns show that all the samples had a hexagonal wurtzite structure belonging to the C_{6v}^4 space group($P6_3mc$) according to the standard JCPDS card(Fig.1). No diffraction peaks of other impurity phases were found in the samples. The 2θ angle of the (002) peak, for the bulk ZnO without stress, was equal to 34.4° in Standard JCPDS card. The 2θ angles of the (002) peak for ZnO sintered at 850 and 1000 °C were larger than 34.4°. Thus the tensile stress in these

samples changed because of the increase in temperature. The authors calculated the ZnO stress, using $\sigma=4.5\times10^{11}(C_0-C)/C_0$, where σ , C , and C_0 were the mean stress in the ZnO, lattice constant of ZnO, and lattice constant of bulk ZnO(standard $C_0=0.5209$ nm). The calculated stress for the samples sintered at 850 and 1000 °C were equal to 0.13 and 0.108, respectively. It indicated that the tensile stress in ZnO decreased with the increase of temperature from 850 to 1000 °C. No diffraction peaks of Ce or other impurity phases were found in sample(Fig.1 curve *d*), suggesting that Ce^{3+} ions had uniformly replaced the Zn^{2+} or entered into interstitial sites in the ZnO lattice. In the Ce-doped ZnO, the major diffraction peaks had shifted slightly toward smaller diffraction angles when compared with those of the standard card(JCPDS No.79-2205, $a=0.3250$ nm, $c=0.5207$ nm). The lattice parameter c calculated from the (002) peak of the Ce-doped ZnO sample was 5.284 nm. The increase in the lattice constant suggested that the larger Ce^{3+} had partly replaced the smaller Zn^{2+} , leading to an increase in the lattice constant. From the XRD patterns of these samples, it could be seen that the peak intensity of sample(Fig.1 curve *d*) decreased greatly and the width broadened. This implied that the Ce^{3+} -doped 1D ZnO nanorods with a smaller average diameter had been synthesized, and the major diffraction peaks had shifted slightly toward smaller diffraction angles when compared with those of the standard card(JCPDS No.79-2205), suggesting that the larger Ce^{3+} had partly replaced the smaller Zn^{2+} .

Fig.2 shows the SEM images of the ZnO nanostructures sintered at different temperatures for 13 h. Nanoparticles with a size of 50—150 nm were obtained at 850 °C, and those with a granular size of about 200—400 nm at 1000 °C. In general, the sizes of the ZnO nanoparticles became bigger with increasing sintering temperature. In Fig.2(C), ZnO shows nanorods rather than polygon granules. The length of the ZnO nanorods was 2—3 μ m and the diameter was in a range of 100—300 nm. The length and the size of the nanorods were quite homogeneous. The annealing temperature had a dominative influence on the microscopic structure and the morphology of ZnO was shown in Figs.2(A—C). Ce-doped ZnO nanorods were obtained *via* annealing at 500 °C, and the lengths of the nanorods reached several micrometers and the diameters about 200 nm, as shown in Fig.2(D).

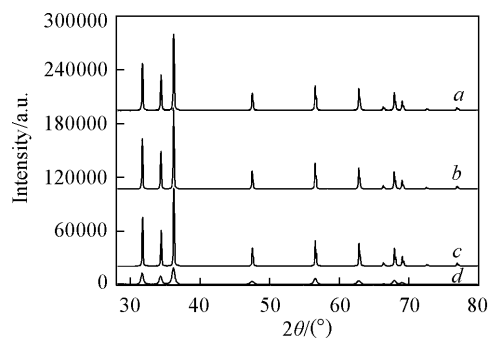


Fig.1 XRD patterns of samples

a. Annealed at 850 °C; *b.* annealed at 1000 °C;
c. annealed at 900 °C; *d.* Ce-doped annealed at 500 °C.

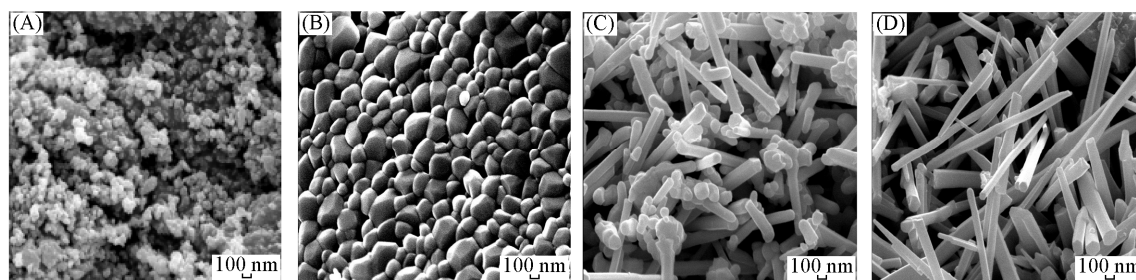


Fig.2 SEM images of ZnO samples

(A) Annealed at 850 °C for 13 h; (B) annealed at 1000 °C for 13 h; (C) annealed at 900 °C for 13 h; (D) Ce-doped ZnO nanorods annealed at 500 °C for 6 h.

3.2 Photoluminescence Properties

Fig.3 illustrates the room-temperature PL spectra of the ZnO samples sintered at 850 and 1000 °C, respectively. Two emission bands could be observed from these samples. One was the near band edge emission in the UV region, which was attributed to free-exciton recombination, and the other was the visible light emission, which was produced by the transition of the excited optical center, from the deep level to the valence level, and such a deep level emission was usually caused by the structural defect and impurities. The spectra showed that the positions and intensities of the PL peaks were both affected by annealing temperature. From Fig.3 curve *a* and curve *b*, it can be seen that the UV emission peak of the ZnO nanoparticles bathochromically shifted from 386 to 389 nm with an increase in annealing temperature from 850 to 1000 °C. This shift of band-gap energy was believed to originate from the change of tensile stress because of lattice distortion. If the tensile was dissipated, the band-gap energy was decreased. Various mechanisms had been proposed for the visible light emission of ZnO. Oxygen vacancies occurred in three different charge states: the neutral oxygen vacancy(Vo), the singly ionized oxygen vacancy(Vo^{\cdot}), and the doubly ionized oxygen vacancy($\text{Vo}^{2\cdot}$). Vanheusden *et al.*^[7] found that only the singly ionized

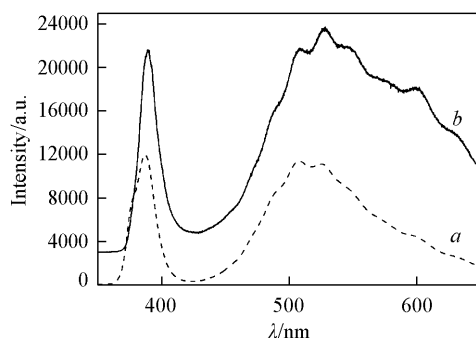


Fig.3 PL spectra of samples

a. ZnO nanoparticles obtained at 850 °C;
b. ZnO granules obtained at 1000 °C.

oxygen vacancies(Vo^{\cdot}) were responsible for the green luminescence from the ZnO. The visible luminescence of ZnO nanoparticles increased as the annealing temperature increased, shown in Fig.3. When the ZnO was heated, it tended to lose oxygen. Though there was no consensus in the literature on the origin of green emission from ZnO, its intensity was commonly related to the density of intrinsic defects(such as oxygen vacancy or Zn interstitial related defects)^[8]. Therefore the increase, in strength, of the visible luminescence of the sample was strongly related to the increase of oxygen vacancies in a high temperature annealing process. Although the oxygen vacancy was an intrinsic donor^[9] in ZnO, the coexistence of another donor(possibly interstitial Zn) with a much higher density should be considered. The diffusivity of Zn in ZnO was much higher than that of O when there was a higher oxygen vacancy at a higher temperature. Hence, Zn atoms could probably diffuse into the particles in interstitial sites. In the investigations, the increase of visible luminescence of ZnO nanoparticles, in strength, was strongly related to the increase of oxygen vacancies and interstitial Zn in a high temperature annealing process.

Fig.4 shows the PL spectra of the ZnO and Ce-doped ZnO nanorods excited by 325 nm at room temperature. The insert shows the absorption spectra. The PL spectra of ZnO nanorods contains a strong UV band peak at 390 nm and a relatively strong and broad green band centered at about 513 nm. Compared with the PL spectrum of ZnO nanorods, the UV emission peak of Ce-doped ZnO nanorods exhibits a large blueshift, whereas, the green emission band is sharply suppressed. The UV emission originates from the excitonic recombination corresponding to the near-band-edge emission of ZnO. The green emission peak is commonly referred to as a deep-level or trap-state emission^[10]. The UV emission peak position of Ce-doped ZnO nanorods shows blueshift compared to that

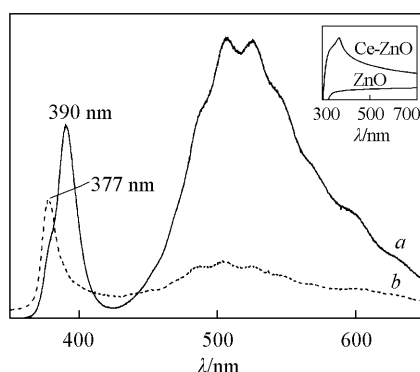


Fig.4 PL of undoped ZnO nanorods prepared at 900 °C (a) and prepared Ce-doped ZnO nanorods at 500 °C (b)

The inset shows their absorption spectra.

of ZnO. This is attributed to the shift of the optical band gap in these nanorods. According to the optical-absorption spectra, pronounced exciton absorption peaks are obvious near the absorption edge. Exciton absorption peak positions of ZnO and Ce-doped ZnO are at 358 and 371 nm, respectively. The change of the optical band gaps of ZnO and Ce-doped ZnO is because of the Burstein-Moss shift^[11]. There are more electrons contributed by the Ce dopant that take up the energy levels located at the bottom of the conduction band. When Ce-doped ZnO samples are excited with a He-Cd laser at 325 nm, excitons take up higher-energy levels at the bottom of the conduction band rather than those of ZnO. Radiative recombination of these excitons will lead to a blueshift of UV emission peak. The lattice strain induced by the lattice distance will also lead to some shift in band gap, although it may not play a major role in the determination of band gap because of the small change in the lattice distances. Decreased UV emission is considered to occur because of an increase in the nanoradiative defect and a decrease in the ZnO nanorod size. A blueshift of the band edge reveals the incorporation of, at least, a part of Ce in the lattice sites. This supports the X-ray results on the incorporation of Ce into the nanorod structure.

From Fig.4 curve *a* and curve *b*, it can be seen that the green emission peak of the Ce-doped ZnO

nanorods is sharply suppressed and broadened. The authors ascribe the decrease of the green emission intensity, after cerium doping, to the decrease in oxygen vacancies and interstitial Zn, in a low temperature annealing process. When Ce ions are incorporated into ZnO and became donors, multi-emission centers are formed, such as, the emission of the electron-hole plasma(EHP), the emission of the electrons of the donors to the valence band, and the intrinsic transition of Ce^{3+} ions. As a result the green emission of Ce-doped ZnO nanorods is broader than that of the undoped ZnO. The PL integrated intensity ratios of the UV emission to the deep-level green emission(I_U/I_D) are 0.69 and 2.06, for undoped ZnO nanorods and Ce-doped ZnO nanorods, respectively. Generally, the intensity ratio of the UV emission band to the visible emission band is regarded as an indicator of the crystallinity of ZnO materials. The higher the ratio is, the better the ZnO crystallinity will be. The strong UV and weak green bands imply a good crystal surface. The increased ratio suggests a good crystal of Ce-doped ZnO nanorods. These results show a great promise for the application of Ce-doped ZnO nanorods with low expense and large quantities of output.

References

- [1] Service R. F., *Science*, **1997**, 276, 895
- [2] Bagnall D. M., Chen Y. F., Zhu Z., *et al.*, *Appl. Phys. Lett.*, **1997**, 70(17), 2230
- [3] Bagnall D. M., Chen Y. F., Zhu Z., *et al.*, *Appl. Phys. Lett.*, **1998**, 73(8), 1038
- [4] Leverenz V. W., *An Introduction to Luminescence of Solids*, Dover, New York, **1968**
- [5] Cheng B., Xiao Y., Wu G., *et al.*, *Appl. Phys. Lett.*, **2004**, 84, 416
- [6] Bofiani Z., Derkowska B., Dalasinski P., *et al.*, *Optics Communications*, **2006**, 267, 433
- [7] Vanheusden K., Warren W. L., Seager C. H., *et al.*, *J. Appl. Phys.*, **1996**, 79(10), 7983
- [8] Vanheusden K., Seager C. H., Warren W. L., *et al.*, *Appl. Phys. Lett.*, **1996**, 68(3), 403
- [9] Mahan G. D., *J. Appl. Phys.*, **1983**, 54(7), 3825
- [10] Vanheusden K., Warren W. L., Seager C. H., *et al.*, *J. Appl. Phys.*, **1996**, 79, 7983
- [11] Burstein E., *Phys. Rev.*, **1954**, 93, 632